

ARTICLE

Received 21 Jan 2014 | Accepted 16 Apr 2014 | Published 27 May 2014

DOI: 10.1038/ncomms4919

OPEN

The refractive index and electronic gap of water and ice increase with increasing pressure

Ding Pan¹, Quan Wan^{1,2} & Giulia Galli²

Determining the electronic and dielectric properties of water at high pressure and temperature is an essential prerequisite to understand the physical and chemical properties of aqueous environments under supercritical conditions, for example, in the Earth interior. However, optical measurements of compressed ice and water remain challenging, and it has been common practice to assume that their band gap is inversely correlated with the measured refractive index, consistent with observations reported for hundreds of materials. Here we report *ab initio* molecular dynamics and electronic structure calculations showing that both the refractive index and the electronic gap of water and ice increase with increasing pressure, at least up to 30 GPa. Subtle electronic effects, related to the nature of interband transitions and band edge localization under pressure, are responsible for this apparently anomalous behaviour.

¹Department of Chemistry, University of California, Davis, California 95616, USA. ²The Institute for Molecular Engineering, University of Chicago, Chicago, Illinois 60637, USA. Correspondence and requests for materials should be addressed to D.P. (email: dpan@ucdavis.edu).

Water is arguably the most important material in the biosphere, as well as a key constituent of the Earth crust and mantle. Its properties have been extensively studied as a function of temperature (T) and pressure (P) for several decades^{1,2}. However, the electronic structure of water under pressure has remained elusive, due to experimental difficulties in measuring absorption processes in wide band gap insulators in diamond anvil cells. The electronic properties of compressed water are key, for example, to understanding electron charge transfer rates in redox reactions^{3,4} occurring in supercritical water¹ and aqueous solutions in the Earth's interior²; such reactions, which depend on both the electronic and static dielectric constant of water, determine the oxidation states of minerals and rocks.

Water was predicted to undergo an insulator-to-metal transition at rather large pressures, estimated between 100 GPa and 5 TPa^{5–8}, although no experimental confirmation has yet been reported. Experimentally, it is difficult to directly establish the variation of the liquid electronic gap as a function of P , which at ambient conditions is outside the optical window of diamond: the optical gap of diamond is 5.4 eV (ref. 9) with the absorption tail as low as ~ 4 eV, and the quasi particle gap of water at ambient conditions is estimated to be 8.7 ± 0.5 eV (refs 10,11) with the optical absorption onset at ~ 7 eV (refs 12,13). Hence, the band gap (E_g) of high pressure ice (a disordered ice phase stable between 3 and ~ 60 GPa (refs 14,15)) has been inferred from measurements of its refractive index, n , which can be obtained by using low energy photons without probing absorption processes¹⁶. In particular, it has been common practice to use a single-oscillator model, for example, the Penn model¹⁷, to relate n and E_g , as in the case of other molecular crystals, notably hydrogen^{18,19}. According to the Penn model, the refractive index n and the electronic gap E_g are inversely correlated: $n^2 = 1 + \frac{(\hbar\omega_p)^2}{E_g^2}$, where ω_p is the plasma frequency. This inverse correlation between n and E_g holds for a broad class of materials^{20,21}.

Zha *et al.*¹⁶ measured the refractive index of ice VII as a function of pressure up to 120 GPa and found that it increased with pressure, similar to the case of solid hydrogen. They found weak dispersion of the refractive index, and its pressure dependence, leading them to conclude that the band gap is preserved to very high pressure, ultimately closing only in the terapascal pressures and well beyond the stability field of ice VII. The refractive index of liquid water has been measured only up to 7 GPa, at $T = 673$ K (ref. 22), while no measurements have yet been reported of its electronic gap in such P - T regime.

Here we report *ab initio* molecular dynamics (MD) simulations of water under pressure and calculations of the refractive index n and the electronic gap E_g in the pressure range 0–30 GPa. The values obtained for the refractive index of ice and water are in good agreement with experiments^{16,22}; however, we find that both n and E_g increase with increasing pressure in the solid and liquid phases. Our results show that a single-oscillator model used to rationalize the electronic properties of many semiconductors and insulators may not be employed to describe water under pressure. We find that, because of subtle but important changes in the localization properties of the valence band edge of water and ice, the strength of inter band transitions depends on pressure. As a consequence n and E_g are not inversely correlated, but exhibit a more complex interdependence, not captured by widely used simple models. Our results are consistent with those of Hermann and Schwerdtfeger²³ who reported an increase of the optical gap of ice under pressure, using calculations based on many body perturbation theory with a fitted dielectric constant.

Results

Refractive index of water and ice. For photon energies ($\hbar\omega$) much smaller than the band gap, absorption processes may be ignored and $n = \sqrt{\epsilon_1}$, where ϵ_1 is the real part of the electronic dielectric constant. For simple semiconductors, the Penn model¹⁷ yields a reasonable approximation of ϵ_1 . The validity of such model may extend beyond simple semiconductors, as suggested by Wemple and DiDomenico²⁰ who showed that $[\epsilon_1(0) - 1]$ is approximately proportional to $1/E_g$ for more than 100 solids and liquids. However, as discussed below, the description of the properties of water and ice requires a more sophisticated level of theory.

Figure 1 reports the calculated refractive index of water and ice, as a function of pressure, and shows that n increases with increasing P along isotherms for both the solid and the liquid. We also show experimental results for ice VII (ref. 16) and water up to 7 GPa (ref. 22). To the best of our knowledge, our results represent the first data obtained for the refractive index of the supercritical liquid above 7 GPa. Indeed, the highly corrosive character of hot, compressed water makes experiments rather challenging at high P and T .

We find good agreement with experiments, especially above 5 GPa, with the deviations present at low pressure ascribed to errors introduced by the use of the Perdew-Burke-Ernzerhof (PBE) functional²⁴. Semi-local functionals have been shown to yield results for water and ice under pressure in better agreement with experiments than at ambient conditions²⁵, for example, for the calculation of the equation of state²⁶ and the dielectric properties^{15,26}. Preliminary calculations of the electronic dielectric constant of water at ambient conditions using the PBE0 (refs 27,28) functional showed a much improved agreement with experiment, yielding $\epsilon_1 = 1.78$ (to be compared with the experimental value of 1.77). The same improvement was also found for the static dielectric constant of ice Ih²⁹. For ice VIII at 30 GPa, we find instead a minor difference of 4% between the electronic dielectric constants obtained by PBE and PBE0.

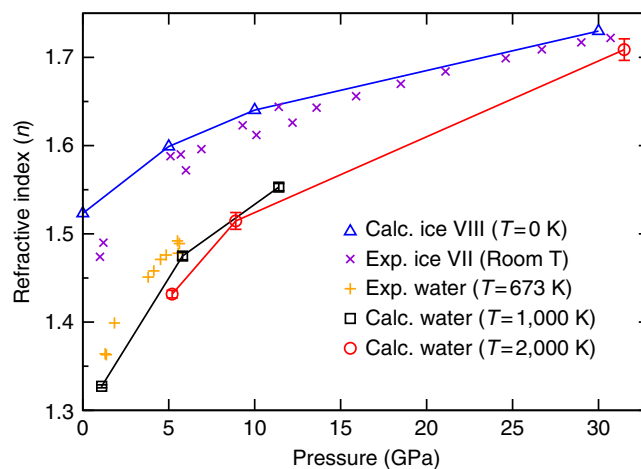


Figure 1 | Refractive indices. Pressure dependence of the refractive index, n , of water and ice. We computed $n = \sqrt{\epsilon_1}$, where ϵ_1 is the real part of the electronic dielectric constant, obtained from *ab initio* simulations (see text). The experimental data for ice VII, obtained with light wavelength of 630 nm, are from ref. 16. The experimental values for water at 673 K are from ref. 22. We note that the statistical fluctuations in the value of n are rather small, indicating that ϵ_1 is largely insensitive to reorientations of the molecules in the fluid and to hydrogen bonding rearrangements, unlike the ionic dielectric constant²⁶. When increasing the temperature from 1,000 to 2,000 K, n showed again moderate variations. The error bars show the s.d. values of the refractive indices of water. Lines are drawn to guide the eyes only. Calculations were conducted for ice VIII instead of VII for computational simplicity, as ice VII is proton disordered.

Electronic gap of water and ice. In Fig. 2, we show the electronic gap of water and ice, computed as the difference between the single particle energies of the conduction band minimum (CBM) and the valence band maximum (VBM) as a function of pressure. We report values obtained with the PBE functional and, in the inset, with the hybrid functional, PBE0 (refs 27,28). In spite of large statistical fluctuations at high T, the trend of an increasing gap with pressure is evident, irrespective of the level of theory used. As well known, the PBE functional underestimates the band gap of water^{11,30}, but the gap variation under pressure is qualitatively the same and quantitatively similar within PBE and PBE0. We expect the rate at which the optical gap increases with pressure be larger than for the electronic gap. Indeed, based on our results for ϵ_1 , we estimated that the exciton binding energy, E_b , of water will be decreased by about 60% in going from ambient pressure to ~ 30 GPa, and that of ice VII/VIII by 40% (The E_b of water at ambient conditions is about 2.4 eV (ref. 30)). Our estimate is based on the relation $E_b = m^*/(m_e \epsilon_1^2 a_0)$, where m^* is the electronic effective mass, m_e the electron mass and a_0 the Bohr radius³¹, and we assumed a negligible variation of the electronic effective mass under pressure, as indicated by our band structure calculations (not shown). Our results for band gaps are consistent with those reported by Hermann and Schwerdtfeger²³ for ice VIII, using many body perturbation theory. These authors used the G_0W_0 approximation and the Bethe-Salpeter equation²³ to compute absorption spectra, with a model dielectric function to approximate the screened Coulomb interaction. In their model, the electronic dielectric constant was an input parameter. Our results are also consistent with those of Boero *et al.*³² who reported an increase in the band gap of supercritical water at 653 K, for densities larger than 0.5 g cm^{-3} , by using *ab initio* MD and the BLYP functional.

Relation between refractive index and band gap. Our calculations showed that both the refractive index and the electronic gap of water and ice increase under pressure, up to at least 30 GPa. They also showed that n of ice is larger than that of the liquid, in spite of the latter having a smaller electronic gap. Thus, the simple inverse correlation between E_g and n used to interpret experiments, and valid for a wide range of substances²⁰, does not hold for water and ice. We show in the following that two reasons are responsible for this apparent anomalous behaviour: an increase in the electronic density

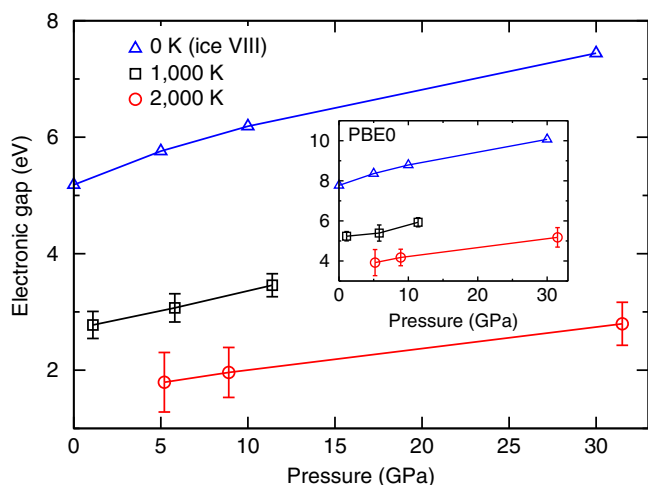


Figure 2 | Electronic gaps. Computed electronic gap of water and ice VIII as a function of pressure at 0, 1,000 and 2,000 K. The calculations were performed using the semilocal density functional, PBE, and in the inset, the hybrid functional PBE0. The error bars show the s.d. values of the band gaps of water. Lines are drawn to guide the eyes only.

with pressure and hence of the plasma frequency $\omega_{\text{ip}}^2 = \frac{4\pi\rho_e e^2}{m_e}$, where ρ_e is the density of valence electrons and e the elementary charge; a change in the localization property of the valence band of the liquid and solid, as P is increased, which in turn is responsible for changes in the strength of interband transitions.

Interestingly, while for ice the increase in ρ_e (and ω_{ip}) counterbalances the increase in E_g and hence $[\epsilon_1(0) - 1]/\rho_e$ decreases under pressure, the corresponding quantity for water shows an increase (see Fig. 3). Ice and water behave as several oxides³³ in exhibiting a positive derivative of the refractive index, with respect to ρ_e . However, for both water and ice the quantity $[\epsilon_1(0) - 1]E_g^2/\rho_e$ is not a constant, as it would be if the Penn model correctly described the relation between the dielectric constant and electronic gap, but it monotonically increases with pressure, at all T considered here.

We therefore adopted a higher level of theory and derived the real part of the electronic dielectric constant in the random phase approximation:

$$\epsilon_1(\omega) = 1 + \frac{e^2}{\pi^2 m_e} \sum_{v,c} \int_{\text{BZ}} d\vec{k} \frac{f_{cv}^\mu(\vec{k})}{\omega_{cv}^2(\vec{k}) - \omega^2} \quad (1)$$

where c and v are the conduction and valence band indices, respectively, and the integral is over the Brillouin Zone (BZ). In the integrand, $f_{cv}^\mu(\vec{k})$ is the oscillator strength in the polarization direction \vec{e}_μ associated with the transition between the bands c and v , and $\hbar\omega_{cv}(\vec{k})$ is the corresponding transition energy. In the case of water, only the Γ point was used in our electronic structure calculations; at zero frequency one has:

$$\epsilon_1(0) = 1 + \frac{8\pi e^2}{V m_e} \sum_{v,c} \frac{f_{cv}^\mu}{\omega_{cv}^2} \quad (2)$$

where V is the volume of the simulation cell. Note that in a single-oscillator model with $\hbar\omega_{cv} = E_g$, Equation 2 reduces to the Penn model, once the oscillator strength sum rule is applied.

The oscillator strength is given by

$$f_{cv}^\mu = \frac{2m_e \omega_{cv}}{\hbar} |\langle c | \vec{e}_\mu \cdot \vec{r} | v \rangle|^2 \propto \epsilon_2(\omega_{cv}) V \omega_{cv}, \quad (3)$$

where $\langle c |$ and $|v\rangle$ denote Kohn-Sham orbitals corresponding to valence (v) and conduction (c) states, and ϵ_2 is the imaginary part of the dielectric function. For v to c transitions right across the

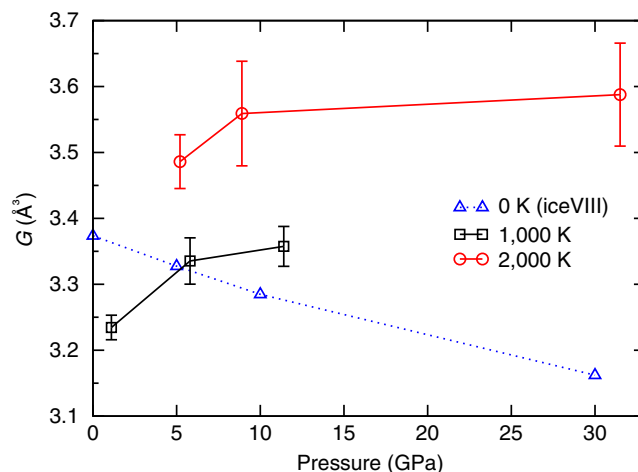


Figure 3 | Volume effect on refractive indices. This figure shows $G = (\epsilon_1(0) - 1)/\rho_e$ as a function of pressure at 0, 1,000 and 2,000 K, where $\epsilon_1(0)$ is the real part of the electronic dielectric constant at zero frequency and ρ_e the valence electron density. The error bars show the s.d. values of the data for water. Lines are drawn to guide the eyes only.

band gap, the oscillator strength is proportional to $[\epsilon_2(\omega_{cv})V\omega_{cv}]$. In Fig. 4 we plotted $\epsilon_2(\omega)V$ of two water configurations at 1,000 K, at ~ 1 GPa and ~ 10 GPa. These are representative of a set of 25 and 55 snapshots analysed for each pressure, extracted from our MD trajectories at equally spaced simulation times; for each of them we found that at $\hbar\omega = E_g$, ϵ_2V is much larger at ~ 10 GPa than at ~ 1 GPa. The oscillator strength of the transitions just across the band gap, which yields the largest contribution to $\epsilon_1(0)$ according to Equation 2, is thus substantially enhanced when the pressure increases from ~ 1 GPa to ~ 10 GPa, and the absorption edge is blue shifted, as expected from our electronic gap calculations. We conclude that it is because of the enhancement of f_{cv}^u , which outweighs the increase of E_g , that the refractive index of water increases under pressure.

We note that local field effects are not included in Equation 1 (ref. 34); they are instead taken into account in our density functional perturbation theory (DFPT)³⁵ calculation of the refractive index (Denote the matrix elements of the static dielectric matrix $\epsilon_{GG'}(0)$, where G and G' are reciprocal lattice vectors; $\epsilon_1^{-1}(0) = [\epsilon_{GG'}(0)]^{-1}|_{G=G'=0}$, implying that $\epsilon_1^{-1}(0)$ is the first element of the inverse dielectric matrix (ref. 35)). However, in Equation 1, $\epsilon_1(0)$ is simply $\epsilon_{00}(0)$ and so called local field effects are neglected³⁴). We verified that neglecting such effects amounts to a negligible error in the calculations of n . In Fig. 5, we compare $\epsilon_1(0)$ of ice VIII, as well as that of high pressure water, obtained with and without local field corrections. The two sets of values are rigidly shifted by only 0.1–0.2 with respect to each other, indicating that none of the trends as a function of pressure reported here is affected by the inclusion of local field effects.

Localization properties of water and ice valence band edges. To understand the changes in the oscillator strength of water under high pressure, we computed the inverse participation ratios (IPRs) of the VBM and CBM orbitals; they are reported in Fig. 6. The IPR is defined as

$$IPR_\alpha = \frac{\frac{1}{N} \sum_{i=1}^N |\psi_\alpha(i)|^4}{\left[\frac{1}{N} \sum_{i=1}^N |\psi_\alpha(i)|^2\right]^2}, \quad (4)$$

where N is the total number of points used to perform integrals over a real space grid, and $\psi_\alpha(i)$ is the wave function associated

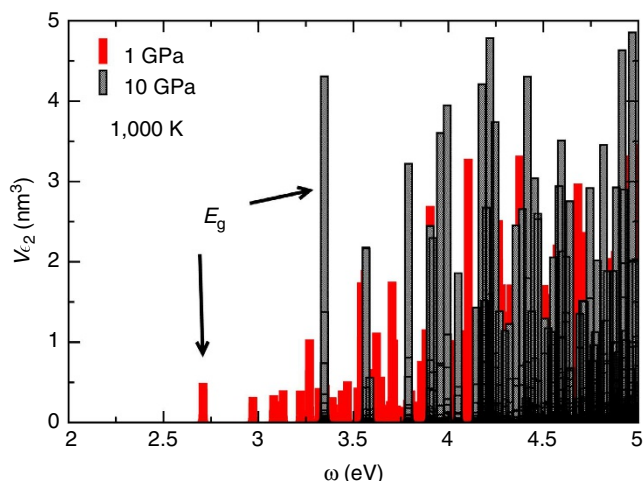


Figure 4 | Oscillator strength of interband transitions. The imaginary part of the electronic dielectric constant of water, ϵ_2 multiplied by the cell volume V as a function of frequency ω at ~ 1 and ~ 10 GPa and 1,000 K. E_g labels the frequencies corresponding to the band gaps of water at ~ 1 and ~ 10 GPa, respectively.

with the band α . The quantity IPR_α yields the statistical variance for the distribution of $|\psi_\alpha|^2$. The larger the IPR, the more localized the wave function. An IPR_α close to 1 indicates a delocalized electronic orbital. Figure 6 shows that, under pressure, as at ambient conditions, the CBM of water is much more delocalized than its VBM³⁷. The interesting finding is that with increasing pressure the localization properties of the CBM are largely unaffected, while those of the VBM change substantially, with a tendency of the VBM to delocalize. The electronic states of ice VIII behave similarly except that the variation of the VBM localization as a function of P is smaller than that of water, as shown in Fig. 6c. As a result, under pressure the spatial overlap between the electron and hole wave functions is enhanced, and the matrix element $\langle c|\vec{e}_\mu \cdot \vec{r}|v\rangle$ increases (see Eq. 3). The fact that the localization of the CBM does not change significantly under pressure, while that of the VBM substantially changes, suggests that the opening of the gap in ice and water under pressure might be mostly due to a change in the position of the VBM.

Experimentally Zha *et al.*¹⁶ measured n as a function of ω and obtained two parameters, E_d and E_0 from the equation $n^2 - 1 = E_d E_0 / (E_0^2 - \hbar^2 \omega^2)$. The fit was then used to conclude that the gap of ice decreases under pressure. Note that in the experiment of ref. 16 when the light wavelength is between 569 to 741 nm, n changes by < 0.05 ; as a result, the effective band gap determined from the single-oscillator model changes little with pressure. It is presumably difficult to estimate E_d and E_0 . The values for E_d and E_0 obtained from the fits gave a predicted closing of the band gap only at ultrahigh pressures (~ 4.5 TPa), well beyond the pressure range of the measurements. We have shown here that state-of-the-art calculations of the electronic structure are essential to properly interpret complex and sophisticated optical experiments and obtain the correct band gap trend under pressure.

Discussion

We reported the first data for the refractive index of supercritical water above 7 GPa and at high temperature. We showed that the refractive index, and the electronic and optical gaps of water and ice increase under pressure, and thus water properties differ

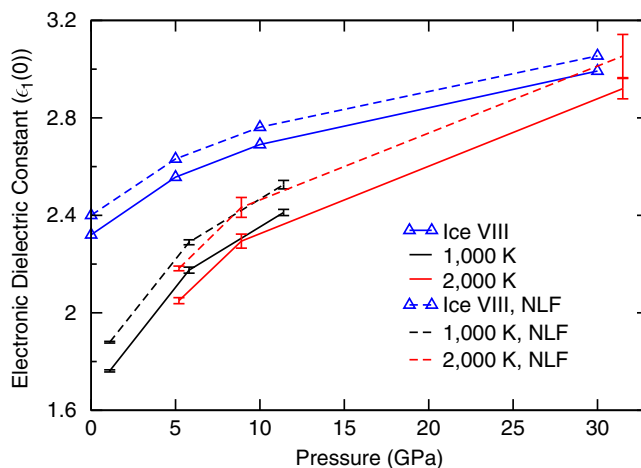


Figure 5 | Local field effects on dielectric constants. The dashed lines show the real part of the electronic dielectric constants of water and ice VIII (0 K) at zero frequency, $\epsilon_1(0)$, obtained from density functional perturbation theory (DFPT) without local field effects (NLF). As a comparison, the results obtained with DFPT and including local field effects (as done in Fig. 1), are shown by the solid lines. The error bars show the s.d. values of the electronic dielectric constants of water.

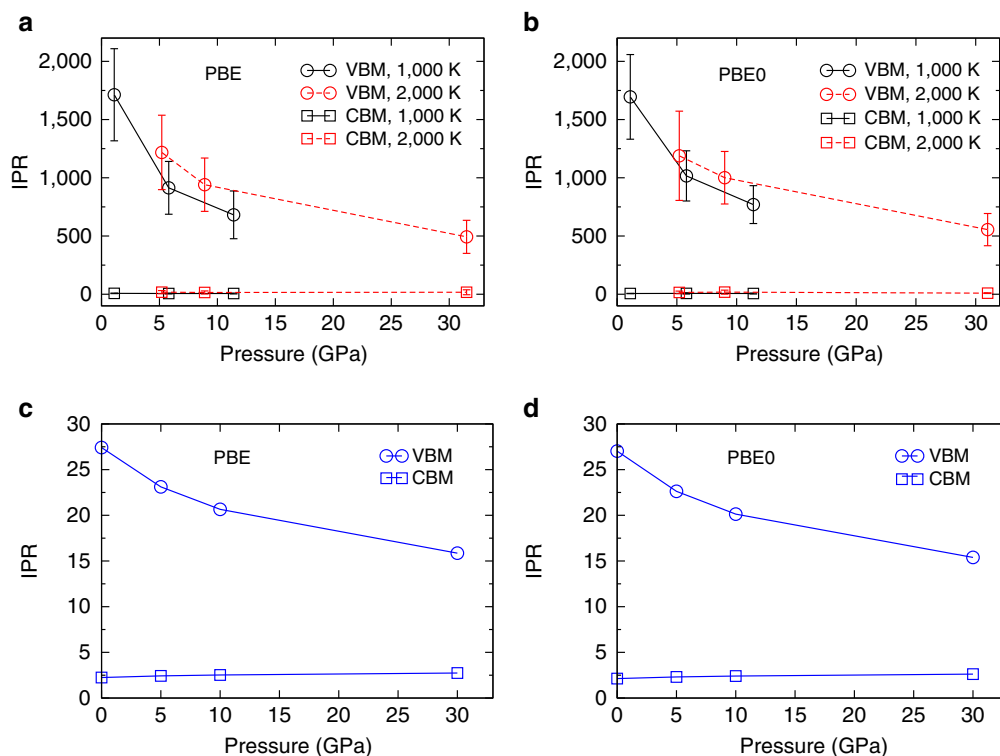


Figure 6 | Localization properties of water conduction and valence band edges. The inverse participation ratios (IPR) of the valence band maximum (VBM, circles) and conduction band minimum (CBM, squares) of (a,b) water and (c,d) ice VIII as a function of pressure. Results of panels b and d were obtained with the hybrid functional PBE0, while those of panels a and c with the semi-local functional PBE. The error bars show the s.d. values of the IPRs of water. Lines are drawn to guide the eyes only.

substantially from those of apolar molecular fluids and solids, for example, hydrogen³⁸, methane^{39,40} and benzene^{41,42}, whose electronic gaps decrease with pressure but refractive indices increase.

We showed that the unusual relationship between n and E_g stems from an enhancement of the strength of interband transitions right across the band gap. This enhancement, in combination with a decrease of the volume, outweighs the increase in the band gap upon compression, and hence the refractive index of water increases with increasing pressure. The behaviour of the interband transition strength originates from the delocalization of the valence band edge, whose overlap with the CBM increases with pressure. Our results showed that the use of simple models, for example, the Penn model¹⁷, to relate measured refractive indices to band gaps of molecular fluids and crystals should be revisited and in general complex electronic structure effects should be taken into account, when predicting values of band gaps. We emphasize that the type of electronic structure calculations reported here allows one to infer the band gap of water from high pressure measurements of the refractive index¹⁶. Measurements of the band gap of water by light absorption or emission are not yet feasible under pressure, in diamond anvil cells; therefore, establishing the correlation between the band gap and the refractive index is a crucial step to infer band gaps from measured dielectric constants. In general, *ab initio* calculations play a key role in interpreting measurements of fluids under pressure, especially in unraveling their electronic structure.

Finally, we note that the results reported here for gaps and dielectric constants are expected to have an important impact in the broad field of water-related science. For example, factors determining the rate of electron transfer in aqueous environments (and hence several chemical reactions occurring in these media) include the refractive index and the static dielectric constant of

the medium³. Hence, knowledge of such quantities is key to predict reorganization energies and electron transfer rates in supercritical water and water under pressure, for example, in the Earth's interior. In addition, the mobility of charges created in water by, e.g., photo-excitation, depends, among other factors, on the exciton binding energy (E_b); our results indicate that E_b decreases under pressure and hence charge mobility is expected to change substantially in supercritical water, with respect to water at ambient conditions, with implications for charge transport under bias, in supercritical conditions.

Methods

Water. We carried out *ab initio* MD simulations of water under pressure as a function of temperature in the Born-Oppenheimer approximation with the Qbox code (version 1.54.2, <http://eslab.ucdavis.edu/software/qbox/>)⁴³. We used 128-molecule unit cells with periodic boundary conditions, plane-wave basis sets and norm conserving pseudopotentials (Gygi, F. Pseudopotential Table, <http://fpm.d.ucdavis.edu/potentials/index.htm>). Atomic trajectories were generated with a plane-wave kinetic energy cutoff of 85 Ry, which was then increased to 220 Ry for the calculation of pressure on selected snapshots²⁶.

Ice VIII. Calculations for ice VIII were conducted by using a 8-molecule unit cell with a plane-wave energy cutoff of 220 Ry and $4 \times 4 \times 3$ k-point mesh and a 96-molecule supercell with a cutoff of 85 Ry and Γ point only.

Electronic structure calculations. Trajectories were generated with the PBE exchange correlation functional²⁴, while electronic gaps and dielectric constants were computed with both the PBE and PBE0 (refs 27,28) functionals on snapshots extracted from PBE trajectories. At the PBE level, the electronic dielectric constant ϵ_1 was calculated using density functional perturbation theory (DFPT)³⁶, as recently implemented in the Qbox code for the calculation of Raman spectra⁴⁴. At the PBE0 level of theory, we instead used an electronic enthalpy functional⁴⁵, where the polarization was computed using maximally localized Wannier functions⁴⁶ with a correction scheme⁴⁷. We calculated the strengths of inter band transitions with the Quantum-expresso package⁴⁸. We used a Gaussian broadening parameter equal to 0.001 eV.

References

- Weingärtner, H. & Franck, E. Supercritical water as a solvent. *Angew. Chem. Int. Ed.* **44**, 2672–2692 (2005).
- Liebscher, A. Aqueous fluids at elevated pressure and temperature. *Geofluids* **10**, 3–19 (2010).
- Chandler, D. in *Computer Simulation of Rare Events and Dynamics of Classical and Quantum Condensed-Phase Systems—Classical and Quantum Dynamics in Condensed Phase Simulations* (eds Berne, B. J., Ciccotti, G., Coke, D. F.) 25–49 (World Scientific, 1998).
- Marcus, R. A. On the theory of oxidation-reduction reactions involving electron transfer. I. *J. Chem. Phys.* **24**, 966–978 (1956).
- Hama, J., Shiomi, Y. & Suito, K. Equation of state and metallization of ice under very high pressure. *J. Phys. Condens. Matter* **2**, 8107 (1990).
- Cavazzoni, C. *et al.* Superionic and metallic states of water and ammonia at giant planet conditions. *Science* **283**, 44–46 (1999).
- Mattsson, T. R. & Desjarlais, M. P. Phase diagram and electrical conductivity of high energy-density water from density functional theory. *Phys. Rev. Lett.* **97**, 017801 (2006).
- Hermann, A., Ashcroft, N. & Hoffmann, R. High pressure ices. *Proc. Natl Acad. Sci.* **109**, 745–750 (2012).
- Clark, C. D., Dean, P. J. & Harris, P. V. Intrinsic edge absorption in diamond. *Proc. R. Soc. London A* **277**, 312–329 (1964).
- Bernas, A., Ferradini, C. & Jay-Gerin, J.-P. On the electronic structure of liquid water: Facts and reflections. *Chem. Phys.* **222**, 151–160 (1997).
- Pham, T. A., Zhang, C., Schwegler, E. & Galli, G. Probing the electronic structure of liquid water with many-body perturbation theory. *Phys. Rev. B* **89**, 060202 (2014).
- Kerr, G. D., Hamm, R. N., Williams, M. W., Birkhoff, R. D. & Painter, L. R. Optical and dielectric properties of water in the vacuum ultraviolet. *Phys. Rev. A* **5**, 2523–2527 (1972).
- Hermann, A., Schmidt, W. G. & Schwerdtfeger, P. Resolving the optical spectrum of water: coordination and electrostatic effects. *Phys. Rev. Lett.* **100**, 207403 (2008).
- Pruzan, P. h., Chervin, J. C. & Canny, B. Stability domain of the ice VIII proton-ordered phase at very high pressure and low temperature. *J. Chem. Phys.* **99**, 9842 (1993).
- Murray, E. D. & Galli, G. Dispersion interactions and vibrational effects in ice as a function of pressure: a first principles study. *Phys. Rev. Lett.* **108**, 105502 (2012).
- Zha, C.-S., Hemley, R. J., Gramsch, S. A., Mao, H.-k. & Bassett, W. A. Optical study of H₂O ice to 120 GPa: Dielectric function, molecular polarizability, and equation of state. *J. Chem. Phys.* **126**, 074506 (2007).
- Penn, D. R. Wave-number-dependent dielectric function of semiconductors. *Phys. Rev.* **128**, 2093–2097 (1962).
- Hemley, R. J., Hanfland, M. & Mao, H. K. High-pressure dielectric measurements of solid hydrogen to 170 GPa. *Nature* **350**, 488 (1991).
- Loubeyre, P., Ocellis, F. & LeToullec, R. Optical studies of solid hydrogen to 320 GPa and evidence for black hydrogen. *Nature* **416**, 613–617 (2002).
- Wemple, S. H. & DiDomenico, Jr M. Behavior of the electronic dielectric constant in covalent and ionic materials. *Phys. Rev. B* **3**, 1338 (1971).
- Kittel, C. *Introduction to Solid State Physics* 8th edn (John Wiley & Sons, 2005).
- Sanchez-Valle, C., Mantegazzi, D., Bass, J. D. & Reusser, E. Equation of state, refractive index and polarizability of compressed water to 7 GPa and 673 K. *J. Chem. Phys.* **138**, 054505 (2013).
- Hermann, A. & Schwerdtfeger, P. Blueshifting the onset of optical UV absorption for water under pressure. *Phys. Rev. Lett.* **106**, 187403 (2011).
- Perdew, J. P., Burke, K. & Ernzerhof, M. Generalized gradient approximation made simple. *Phys. Rev. Lett.* **77**, 3865 (1996).
- Galli, G. & Pan, D. A closer look at supercritical water. *Proc. Natl Acad. Sci. USA* **110**, 6250–6251 (2013).
- Pan, D., Spanu, L., Harrison, B., Sverjensky, D. A. & Galli, G. Dielectric properties of water under extreme conditions and transport of carbonates in the deep earth. *Proc. Natl Acad. Sci. USA* **110**, 6646–6650 (2013).
- Adamo, C. & Barone, V. Toward reliable density functional methods without adjustable parameters: The PBE0 model. *J. Chem. Phys.* **110**, 6158 (1999).
- Gygi, F. & Duchemin, I. Efficient computation of Hartree-Fock exchange using recursive subspace bisection. *J. Chem. Theory Comput.* **9**, 582–587 (2012).
- Schönherr, M., Slater, B., Hutter, J. & VandeVondele, J. Dielectric properties of water ice, the ice Ih/XI phase transition and an assessment of DFT. *J. Phys. Chem. B* **118**, 590–596 (2014).
- Garbuio, V., Cascella, M., Reining, L., Sole, R. D. & Pulci, O. Ab initio calculation of optical spectra of liquids: many-body effects in the electronic excitations of water. *Phys. Rev. Lett.* **97**, 137402 (2006).
- Dvorak, M., Wei, S.-H. & Wu, Z. Origin of the variation of exciton binding energy in semiconductors. *Phys. Rev. Lett.* **110**, 016402 (2013).
- Boero, M., Terakura, K., Ikeshoji, T., Liew, C. C. & Parrinello, M. Water at supercritical conditions: A first principles study. *J. Chem. Phys.* **115**, 2219 (2001).
- Waxler, R. M. & Cleek, G. W. The effect of temperature and pressure on the refractive index of some oxide glasses. *J. Res. Natl Bur. Stand. Sect. A* **77**, 755–763 (1973).
- Wiser, N. Dielectric constant with local field effects included. *Phys. Rev.* **129**, 62–69 (1963).
- Baroni, S., de Gironcoli, S., Dal Corso, A. & Giannozzi, P. Phonons and related crystal properties from density-functional perturbation theory. *Rev. Mod. Phys.* **73**, 515–562 (2001).
- Ping, Y., Rocca, D. & Galli, G. Electronic excitations in light absorbers for photoelectrochemical energy conversion: first principles calculations based on many body perturbation theory. *Chem. Soc. Rev.* **42**, 2437–2469 (2013).
- Laasonen, K., Sprik, M., Parrinello, M. & Car, R. 'Ab initio' liquid water. *J. Chem. Phys.* **99**, 9080 (1993).
- García, A. *et al.* Dielectric properties of solid molecular hydrogen at high pressure. *Phys. Rev. B* **45**, 9709–9715 (1992).
- Lin, H., Li, Y.-l., Zeng, Z., Chen, X.-j. & Lin, H. Structural, electronic, and dynamical properties of methane under high pressure. *J. Chem. Phys.* **134**, 064515 (2011).
- Hebert, P., Polian, A., Loubeyre, P. & Le Toullec, R. Optical studies of methane under high pressure. *Phys. Rev. B* **36**, 9196–9201 (1987).
- Wen, X.-D., Hoffmann, R. & Ashcroft, N. Benzene under high pressure: a story of molecular crystals transforming to saturated networks, with a possible intermediate metallic phase. *J. Am. Chem. Soc.* **133**, 9023–9035 (2011).
- Takagi, T. & Teranishi, H. Refractive index of liquids under high pressure. *J. Chem. Eng. Data* **27**, 16–18 (1982).
- Gygi, F. Architecture of qbox: A scalable first-principles molecular dynamics code. *IBM J. Res. Dev.* **52**, 137–144 (2008).
- Wan, Q., Spanu, L., Galli, G. A. & Gygi, F. Raman spectra of liquid water from ab initio molecular dynamics: vibrational signatures of charge fluctuations in the hydrogen bond network. *J. Chem. Theory Comput.* **9**, 4124–4130 (2013).
- Souza, I., Iniguez, J. & Vanderbilt, D. First-principles approach to insulators in finite electric fields. *Phys. Rev. Lett.* **89**, 117602 (2002).
- Marzari, N., Mostofi, A., Yates, J., Souza, I. & Vanderbilt, D. Maximally localized Wannier functions: Theory and applications. *Rev. Mod. Phys.* **84**, 1419–1475 (2012).
- Stengel, M. & Spaldin, N. Accurate polarization within a unified Wannier function formalism. *Phys. Rev. B* **73**, 075121 (2006).
- Giannozzi, P. *et al.* QUANTUM ESPRESSO: a modular and open-source software project for quantum simulations of materials. *J. Phys. Condens. Matter* **21**, 395502 (2009).

Acknowledgements

We thank F. Gygi, M. Govoni and Y. Ping for many useful discussions and R. Hemley for a critical reading of the manuscript. This work was supported by Department of Energy (DOE), Computer Materials and Chemical Sciences Network, under Grant DE-SC0005180, and by the Sloan Foundation through the Deep Carbon Observatory. Part of this work was carried out using computational resources from the Extreme Science and Engineering Discovery Environment (XSEDE), provided by the National Institute for Computational Sciences (NICS) under Grant TG-MCA06N063, which is funded by the National Science Foundation; and resources at Lawrence Berkeley National Laboratory, NERSC, supported by DOE under Contract No. DE-FG02-06ER46262.

Author contributions

D.P. and G.G. designed the research. Most of the calculations were performed by D.P., with contributions from all authors. Q.W. implemented a Density Functional Perturbation Theory (used for the calculation of the dielectric constants) into the Qbox code. All authors contributed to the analysis and discussion of the data and the writing of the manuscript.

Additional information

Supplementary Information accompanies this paper at <http://www.nature.com/naturecommunications>

Competing financial interests: The authors declare no competing financial interests.

Reprints and permission information is available online at <http://www.nature.com/reprints/index.html>.

How to cite this article: Pan D. *et al.* The refractive index and electronic gap of water and ice increase with increasing pressure. *Nat. Commun.* **5**:3919 doi: 10.1038/ncomms4919 (2014).



This work is licensed under a Creative Commons Attribution-NonCommercial-ShareAlike 3.0 Unported License. The images or other third party material in this article are included in the article's Creative Commons license, unless indicated otherwise in the credit line; if the material is not included under the Creative Commons license, users will need to obtain permission from the license holder to reproduce the material. To view a copy of this license, visit <http://creativecommons.org/licenses/by-nc-sa/3.0/>